Path-Based Channel Estimation for Acoustic OFDM Systems: Real Data Analysis

Amir Tadayon *Student Member, IEEE* and Milica Stojanovic, *Fellow, IEEE*
Northeastern University, Boston, MA, USA

***Abstract*—We address detection of acoustic OFDM signals using a channel estimation method based on a physical model of multipath propagation rather than an equivalent sample-spaced model. The path identification (PI) algorithm focuses on explicit estimation of delays and complex amplitudes of the channel paths. We apply this algorithm, along with the conventional least squares (LS) and orthogonal matching pursuit (OMP) to a set of signals recorded over a mobile acoustic channel. We demonstrate excellent performance of the PI algorithm and show that its complexity is considerably lower than that of the OMP algorithm. The PI algorithm consistently outperforms the conventional LS and compares favorably with the OMP algorithm in terms of the mean-squared data detection error observed for a varying number of OFDM carriers and receiver array configurations.**

I. Introduction

Channel estimation for multicarrier (OFDM) acoustic systems has been studied extensively in recent years [1]–[3]. These studies have recognized the fact that acoustic channels are sparse, and have put forth a number of channel estimation algorithms that take advantage of this fact.

The conventional least squares (LS) algorithm targets estimation of sample-spaced channel taps, with sampling at the basic rate equal to the system bandwidth. With the advent of sparse estimation, focus has shifted to the sparse nature of physical multipath channels, as it can be leveraged to improve channel estimation to either work with fewer pilot symbols or to achieve better noise suppression. In [1], a channel estimator based on the greedy orthogonal matching pursuit (OMP) using dictionaries with finer delay resolution (sub-sample spacing) has been addressed. The OMP algorithm identifies the dominant channel taps sequentially, selecting at each iteration one column of the over-complete dictionary that correlates best with the approximation residual from the previous iteration, and recomputing the coefficients by solving a constrained least-squares problem to fit the observations [4], [5]. This method showed a marked improvement in application to both synthetic and real data; however, the associated computational complexity, which comes from using finer over-complete dictionaries, is not negligible. Additionally, a strong effect of diminishing returns is observed as the granularity (oversampling ratio) is increased [1].

To address these issues, we formulate the problem of sparse channel estimation in a different manner, capitalizing on a physical model of multipath propagation [6]. The resulting approach, termed path identification (PI), targets a continuum of path delays, eliminating the sample-spaced model and focusing instead on processing a transformed version of the signal observed over all the carriers spanning the system bandwidth. Unlike the sparse identification methods with over-complete dictionaries, the resolution and coverage in delay that the PI algorithm provides can be increased without a prohibitive cost in complexity.

While [6] illustrates the benefits of path identification through simulation, in this paper we present an extensive analysis of a real-data set obtained over a mobile acoustic channel. The experimental signals, designed with a varying number of carriers $(256-2048)$ and QPSK modulation within a 5 kHz acoustic bandwidth, are transmitted repeatedly over a multi-hour period during which the transmitting station moves at varying speeds up to 1.5 m/s. The PI algorithm is applied to the recorded signals, and its performance is compared to that of conventional LS and OMP. The PI algorithm outperforms LS, and offers performance comparable to that of OMP at considerably lower computational complexity.

The rest of the paper is organized as folows. In Sec. II, we introduce the system and channel model. Sec. III briefly outlines the path identification method. Sec. IV contains the results of experimental data processing. We conclude in Sec. V.

II. System and Channel Model

We consider an OFDM system with K carriers within a total bandwidth B. Let f_0 and $\Delta f = B/K$ denote the first carrier frequency and carrier spacing, respectively. We assume the use of either a cyclic prefix or zero-padding in the transmitter along with the overlap-and-add procedure at the receiver [7]. We also assume that the channel is slowly varying, such that the time-variation within a single OFDM block of duration $T = 1/\Delta f$ can be neglected. In an acoustic channel, this assumption can hold only if proper front-end resampling is performed to compensate for the motion-induced Doppler effects. We will comment on this issue later.

Under these assumptions, the signal on the kth carrier can be described as

$$y_k = d_k H_k + z_k, \quad k = 0, \ldots, K-1 \tag{1}$$

where d_k is the transmitted data symbol that belongs to a unit-amplitude PSK alphabet, H_k is the channel frequency response at the kth carrier, and z_k is the circularly symmetric, zero-mean additive Gaussian noise of variance σ_z^2.

We model the propagation channel during of one OFDM block as

$$H(f) = \sum_k h_p e^{-2\pi i f \tau_p} \tag{2}$$

where h_p and τ_p represent the path gains and delays, respectively. At the carrier frequency $f_k = f_0 + k\Delta f$, we then have

$$H(f_k) = H_k = \sum_p c_p e^{-2\pi i k \Delta f \tau_p} \tag{3}$$

where $c_p = h_p e^{-2\pi i f_0 \tau_p}$.

III. Path Identification Algorithm

In this section, we briefly discuss the path identification (PI) algorithm for channel estimation proposed in [6].

Referring to (2) as the physical channel model, we re-write it in a matrix-vector format as

$$\mathbf{H} = \sum_p c_p \mathbf{s}_K(2\pi\Delta f \tau_p) \tag{4}$$

where $\mathbf{s}_K(2\pi\Delta f\tau) = \begin{bmatrix}1 & e^{-2\pi i \Delta f \tau} & \cdots & e^{-2\pi i (K-1)\Delta f \tau}\end{bmatrix}^T$ is referred to as the steering vector at an arbitrary delay τ.

Assuming without the loss of generality that all K data symbols are available for channel estimation (e.g. correct symbol decisions, or all-pilots in an initial block), the input to the channel estimator is given by $x_k = y_k/d_k$, i.e.

$$\mathbf{x} = \mathbf{H} + \mathbf{z} \tag{5}$$

where $\mathbf{z}$ represents an equivalent noise vector.

Consider now the following operation performed on the noisy channel observation $\mathbf{x}$:

$$\begin{aligned} r(\tau) &= \frac{1}{K}\mathbf{s}_K^H(2\pi\Delta f\tau)\mathbf{x} \\ &= \sum_p c_p g_K\left(2\pi\Delta f(\tau-\tau_p)\right) + w(\tau) \quad \tau \in \tau_{obs} \end{aligned} \tag{6}$$

where

$$g_K(\phi) = \frac{1}{K}\sum_{k=0}^{K-1} e^{ik\phi} \tag{7}$$

is a known signature function and $w(\tau)$ is complex Gaussian noise with variance $\sigma_w^2 = \sigma_z^2/K$. This operation corresponds to steering across the carriers.

The interval τ_{obs} is a pre-set interval that captures the multipath spread. In a digital implementation, an arbitrary resolution is used, e.g. $\Delta\tau = T/IK$, where I represents the resolution factor, i.e. the increase in resolution over the standard sample spacing $1/B = T/K$. The total length of the observation interval is $L = \lceil T_g B \rceil$, where T_g is the guard interval which is at least as long as the multipath spread.

The signal $r(\tau)$ serves as the input to the PI algorithm. The algorithm operates recursively, identifying at each iteration the delay of the next-strongest path in a manner similar to matching pursuit. The algorithm can be set to run either for a pre-specified number of channel paths N_p (sparsity level) or a pre-defined residual error threshold η.

The formal steps of the PI algorithm are summarized in Algorithm 1. The last step of the algorithm represents a refinement in which a least squares problem is solved for possible improvement in estimating the path gains c_p. This step is optional.

Algorithm 1 PI algorithm

Input: $\mathbf{x}$, N_p (or η)
Output: $\hat{\mathbf{H}}$

1: $r_0(\tau) = r(\tau) = \frac{1}{K}\mathbf{s}_K^H(2\pi\Delta f\tau)\mathbf{x}$ {*initialization step*}
2: **while** $p \le N_p$ (or $|r_p(\tau)| > \eta \max_\tau |r(\tau)|$) **do**
3: $\hat{\tau}_p = \arg\max_\tau |r_p(\tau)|$
4: $\hat{c}_p = r_p(\hat{\tau}_p)$
5: $r_{p+1}(\tau) = r_p(\tau) - \hat{c}_p g_K\left(2\pi\Delta f(\tau - \hat{\tau}_p)\right.$
6: **end while**
7: $\hat{\mathbf{S}} = \begin{bmatrix}\mathbf{s}_K(2\pi\Delta f\hat{\tau}_1) & \cdots & \mathbf{s}_K(2\pi\Delta f\hat{\tau}_{N_p})\end{bmatrix}$
8: $\hat{\mathbf{c}} = \left(\hat{\mathbf{S}}^H\hat{\mathbf{S}}\right)^{-1}\hat{\mathbf{S}}^H\mathbf{x}$ {*refinement step*}
9: **return** $\hat{\mathbf{H}} = \hat{\mathbf{S}}\hat{\mathbf{c}}$

The running time of the PI algorithm is dominated by the initialization step which takes ILK floating point operations (flops). Capitalizing on the fact that the signature function $g_K(\cdot)$ is known, the operations within the loop take only IL flops per iteration. The (optional) refinement step takes KN_p^2 flops. The total complexity of the PI algorithm is thus $O(ILK) + O(N_pIL) + O(KN_p^2)$. Compared to $O(N_tIK\log_2 IK) + O(\frac{5}{2}KN_t^2)$ for the OMP algorithm, where N_t is the sparsity level of the channel tap vector, this represents an improvement, which we will illustrate numerically in the following section.

In a multichannel receiver with M_r spatially distributed elements, one FFT demodulator is associated with each input channel. Using the model (1) then yields the M_r-element received signal vector

$$\mathbf{y}_k = d_k\mathbf{H}_k + \mathbf{z}_k, \quad k = 0, \ldots, K-1 \tag{8}$$

where $\mathbf{H}_k$ and $\mathbf{z}_k$ contain the relevant channel and noise components, respectively. Assuming that the channels observed across the receiver array are uncorrelated, maximum ratio combining (MRC) yields the data estimate[1]

$$\hat{d}_k = \frac{1}{\|\hat{\mathbf{H}}_k\|_2^2}\hat{\mathbf{H}}_k^H\mathbf{y}_k, \quad k = 0, \ldots, K-1 \tag{9}$$

IV. Experimental Result

To asses the system performance, we focus on the experimental data from the Mobile Acoustic Communication Experiment (MACE'10) which took place off the coast of Martha's Vineyard, Massachusetts, in June 2010. The experimental signals, whose parameters are given in Table I, were transmitted using the acoustic frequency range between 10.5 kHz and 15.5 kHz. The receiver array of 12 equally-spaced elements spanning a total linear aperture of 1.32 m was suspended at the depth of 40 m and the transmitter was towed at the depth of 40-60 m. The water depth was approximately 100 m, and the transmission distance varied between 3 km and 7 km. More details about the experiment can be found in [8].

The experiment consisted of multiple repeated transmissions, each containing all the OFDM signals listed in Table I. There was a total of 52 transmissions spanning 3.5 hours of

[1]Conjugate-transpose is denoted by $(\cdot)^H$.

recording. During this time, the transmitting station moved away and towards the receiving station, at varying speeds ranging from 0.5 m/s to 1.5 m/s. The results provided in this section are obtained from all 52 transmissions.

TABLE I
MACE'10 SIGNAL PARAMETERS. THE GUARD INTERVAL IS $T_g = 16$ msec. THE BANDWIDTH EFFICIENCY IS CALCULATED ASSUMING 136 PILOTS.

number of carriers K	256	512	1024	2048
number of blocks per frame N_B	32	16	8	4
carrier spacing Δf [Hz]	19.2	9.6	4.8	2.4
bit rate [kbps]	7.5	8.5	9	9.4
bandwidth efficiency [bps/Hz]	0.72	1.28	1.62	1.8

A. Frequency Offset Estimation

Relative motion between the transmitter and receiver introduces Doppler effect which causes non-uniform frequency shifting across the acoustic signal bandwidth. For the relative transmitter/receiver velocity v and the propagation speed c (nominally 1500 m/s), Doppler scaling occurs at the rate $a = v/c$. For the signals at hand (MACE'10), where the relative speed between the transmitter and receiver varies from 0.5 to 1.5 m/s, the magnitude of the Doppler scale a is between 3×10^{-4} and 10^{-3}, leading to Doppler shifting of the lowest carrier by af_0, which is between $0.65\Delta f$ and $2.15\Delta f$ for OFDM signal with $K = 1024$ carriers and carrier spacing $\Delta f = 4.8$ Hz. The corresponding Doppler shift for the highest carrier in the OFDM signals with $K = 1024$ is between $1.1\Delta f$ and $3.2\Delta f$.

Doppler scaling is effectively see as a time-varying channel distortion, which adversely affects the performance of OFDM systems as it causes loss of orthogonality between the carriers. To mitigate the resulting distortion, front-end resampling must be performed [8], [9]. Coarse resampling is typically performed on an entire frame of OFDM blocks, and may leave individual blocks within a frame exposed to different frequency offsets. These offsets, if left uncompensated, would have a detrimental impact on data detection.

We treat the frequency offset using a hypothesis testing approach. The approach is based on differentially coherent detection which keeps the complexity at its minimum and requires only a very low pilot overhead. In this approach, several hypothesized values of the frequency offset are used, e.g. in steps of $\Delta f/10$, and differential maximal ratio combining is performed for each hypothesized value. The squared error on the pilot carriers is finally measured, and the hypothesis corresponding to the smallest error is identified. The corresponding frequency offset is used to compensate for the Doppler distortion before feeding the signal to the FFT demodulator.

B. Results

We compare the performance of the PI channel estimation method in terms of data detection mean-squared error (MSE) and average execution time $\bar{T}_{exe}$ which is deemed a practical indicator of the algorithm complexity. We also report on the estimated cumulative density function (CDF) of the MSE measured in each signal frame. Furthermore, adding synthetic noise to the received signal enables us to compare the MSE performance versus signal-to-noise ratio (SNR).

The MSE is measured in the n-th block of the i-th frame as

$$MSE^i(n,K) = \frac{1}{K}\sum_{k=0}^{K-1} |d_k(n) - \hat{d}_k^i(n)|^2 \qquad (10)$$

and the MSE per frame is obtained as

$$MSE^i(K) = \frac{1}{N_B}\sum_{n=0}^{N_B-1} MSE^i(n,K) \qquad (11)$$

The average over all 52 frames is

$$\bar{MSE}(K) = \frac{1}{52}\sum_{i=1}^{52} MSE^i(K) \qquad (12)$$

Note that due to the random channel variation and a finite number of measurements, each of these quantities is a random variable.

Fig. 1 illustrates the average MSE performance as a function of the number of carriers K (log scale). Each point in this plot is obtained by averaging over all carriers, blocks and 52 frames transmitted. This result shows that the PI algorithm terminated based on a pre-defined sparsity level outperforms the LS and OMP algorithms by 2 and 1 dB, respectively, when $\log_2(K) = 8, 9$ and 10. When $\log_2(K) = 11$ both the PI and OMP experience a deterioration in performance, which can be explained by the increased block duration that nudges the temporal coherence of the channel. Fig. 1 also shows that increasing the resolution factor I from 1 to 2 improves the performance of both the PI and OMP algorithms. Further increase from 2 to 4 does not bring as much improvement.

Fig 2 shows the performance of the algorithms in terms of the average execution time. The OMP algorithm is implemented using the fast Fourier transform (FFT) for calculating the correlation between the residual and the columns of the over-complete Discrete Time Fourier (DFT) dictionary, and the modified-Gram-Schmidt algorithm for solving the constrained LS problem in each iteration. Clearly, the PI algorithm has lower complexity than the OMP algorithm. It thus enables operation with a greater number of carriers, thus increasing the bandwidth efficiency at a lower computational complexity. Lower computational complexity and better MSE performance make the PI algorithm a good practical candidate for channel estimation in coherent acoustic OFDM systems.

Fig. 3 illustrates the estimated cumulative density function of the MSE per block. This result refers to $K = 1024$ carries and includes the 52 frames transmitted over 3.5 hours. The threshold-based PI algorithm delivers MSE below -15 dB for 84% of the OFDM blocks, while the threshold-based OMP algorithm delivers MSE below -15 dB for 74% of the OFDM blocks.

Fig. 4 illustrates the MSE performance as a function of the number of receiving elements M_r which are chosen among the 12 available elements. For $M_r \leq 6$, two sets

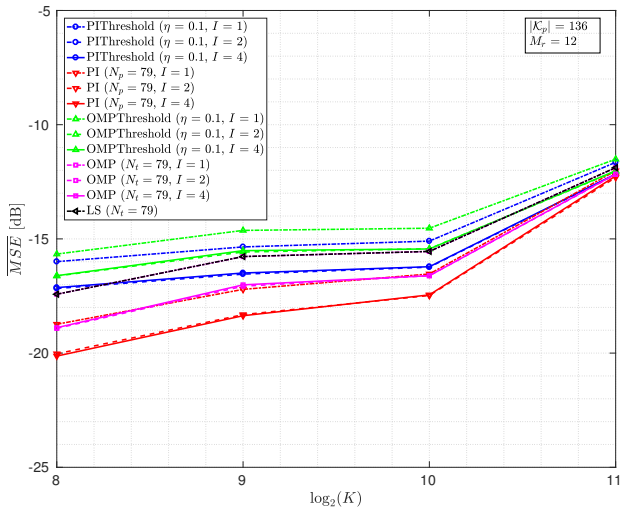

Fig. 1. Average MSE versus the number of carriers K. For both the PI and OMP algorithms, two stopping criteria have been chosen, one based on the sparsity level (for PI $N_p = 79$ and for OMP $N_t = 79$) and one based on a threshold $\eta = 0.1$. The resolution factors I used in the PI and OMP algorithms are 1, 2, and 4. For the case with $K = 1024$, $I = 4$ and $\eta = 0.1$, the PI and OMP algorithms return about 25 coefficients. All 12 receivers are used to perform MRC (9).

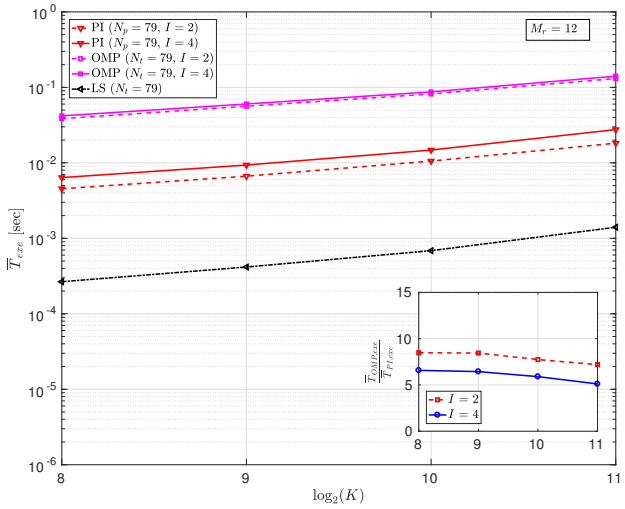

Fig. 2. Average execution time as a function of the number of carriers (log scale) and the resolution factor $I = 2$ and 4. Execution time values represent the average over all blocks, 12 receive elements and 52 transmitted frames. The inset shows the ratio of the execution time of OMP algorithm to that of PI algorithm as a function of the number of carriers for $I = 2, 4$.

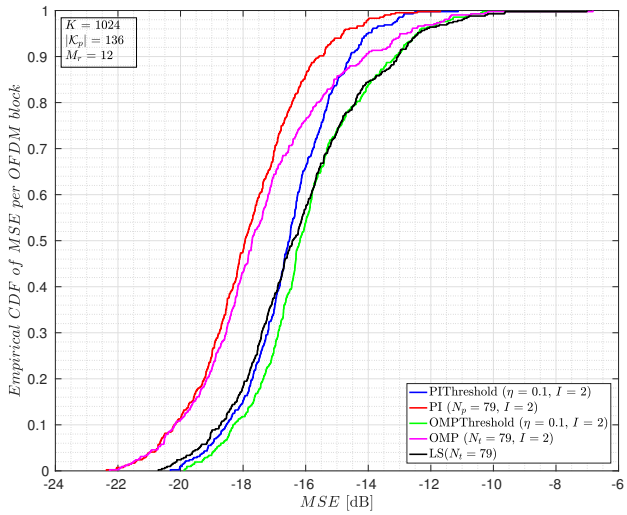

Fig. 3. The estimated CDF of the MSE for various channel estimation techniques. The CDFs reflect all 52 transmission with $K = 1024$ carriers during MACE'10. The resolution factor for the PI and OMP algorithms is $I = 2$. The conventional LS technique delivers MSE below -15 dB for only 73.5% of OFDM blocks. The OMP algorithm with $I = 2$ improves the performance by delivering MSE below -15 dB for 85% of the blocks. The PI algorithm outperforms both by delivering MSE below -15 dB for 94% of the blocks at lower complexity compared to the OMP algorithm.

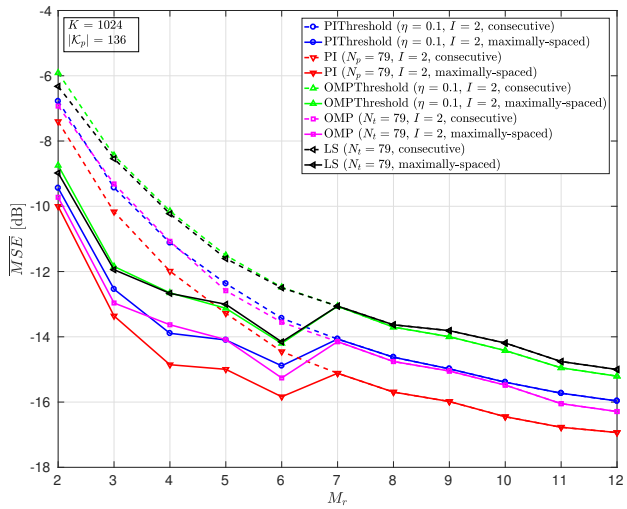

Fig. 4. Average MSE of the conventional LS, OMP and PI algorithms versus the number of receiving elements. The number of carriers and the resolution factor are 1024 and 2, respectively. For $M_r \leq 6$, two sets of receiving elements are chosen, one with consecutive elements and one with maximally-spaced elements.

of receiving elements among the 12 available elements are chosen, one with consecutive elements and the other with maximally equally spaced elements. As one would expect, using maximally equally spaced elements is the better choice. The PI algorithm outperforms the LS and OMP algorithms for all the configurations considered.

Adding synthetic noise to the received signal, we also compare the MSE performance of the algorithms as a function of the input SNR for the case with $K = 1024$ carriers and the oversampling factor $I = 2$. As shown in Fig. 5, the PI algorithms outperforms the other algorithms, and notably so in the high SNR regime ($SNR \geq 10$ dB).

V. Conclusion

Within the framework of OFDM signal detection, we investigated a channel estimation method that operates on the transformed version of the input signal to identify the dominant propagation paths. Unlike the conventional methods, path identification considers a continuum of delays and allows for increasing the delay resolution without undue penalty on complexity.

We presented a comparative performance analysis using experimental signals recorded over a mobile acoustic channel. Our results show that the PI algorithm consistently outper-

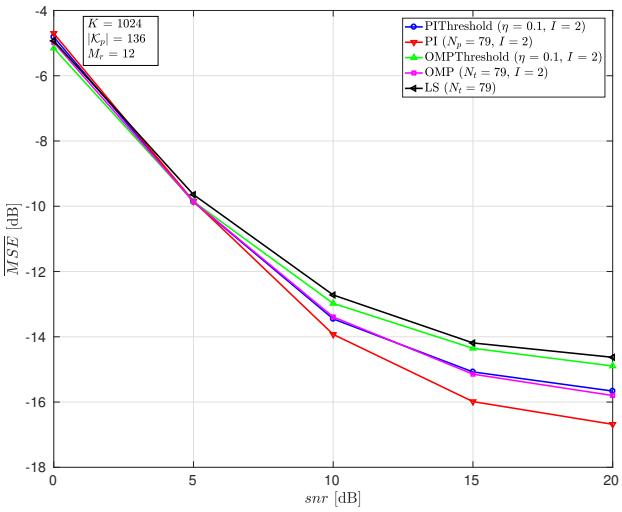

Fig. 5. Average MSE of the conventional LS, OMP and PI algorithms versus the input SNR. The number of carriers and the resolution factor are 1024 and 2, respectively. The number of receiver elements used to perform maximal ratio combining is $M_r = 12$.

forms the conventional LS and offers a performance comparable to that OMP albeit with much lower computational complexity. Specifically, the PI algorithm is on average 8 times faster than the OMP algorithm. Such an advantage is of paramount importance for practical implementation of high data rate acoustic OFDM systems. In terms of performance, the PI algorithm delivered an average MSE below -15 dB for 94% of OFDM blocks, while the OMP and LS did so for 84% and 74% of OFDM blocks, respectively.

REFERENCES

[1] C. R. Berger, S. Zhou, J. C. Preisig, and P. Willett, "Sparse channel estimation for multicarrier underwater acoustic communication: From subspace methods to compressed sensing," *IEEE Trans. Signal Process.*, vol. 58, no. 3, pp. 1708–1721, Mar. 2010.

[2] A. Radosevic, R. Ahmed, T. M. Duman, J. G. Proakis, and M. Stojanovic, "Adaptive OFDM modulation for underwater acoustic communications: Design considerations and experimental results," *IEEE J. Ocean. Eng.*, vol. 39, no. 2, pp. 357–370, Apr. 2014.

[3] T. Kang and R. A. Iltis, "Iterative carrier frequency offset and channel estimation for underwater acoustic OFDM systems," *IEEE J. Sel. Areas Commun.*, vol. 26, no. 9, pp. 1650–1661, Dec. 2008.

[4] W. Li and J. C. Preisig, "Estimation of rapidly time-varying sparse channels," *IEEE J. Ocean. Eng.*, vol. 32, no. 4, pp. 927–939, Oct. 2007.

[5] J. A. Tropp and A. C. Gilbert, "Signal recovery from random measurements via orthogonal matching pursuit," *IEEE Trans. Inf. Theory*, vol. 53, no. 12, pp. 4655–4666, Dec. 2007.

[6] M. Stojanovic and S. Tadayon, "Estimation and tracking of time-varying channels in OFDM systems," in *Proc. 52nd Annu. Allerton Conf. Commun. Control Comput.*, Sep. 2014, pp. 116–122.

[7] B. Muquet, Z. Wang, G. B. Giannakis, M. de Courville, and P. Duhamel, "Cyclic prefixing or zero padding for wireless multicarrier transmissions?" *IEEE Trans. Commun.*, vol. 50, no. 12, pp. 2136–2148, Dec. 2002.

[8] Y. M. Aval and M. Stojanovic, "Differentially coherent multichannel detection of acoustic OFDM signals," *IEEE J. Ocean. Eng.*, vol. 40, no. 2, pp. 251–268, Apr. 2015.

[9] B. Li, S. Zhou, M. Stojanovic, L. Freitag, and P. Willett, "Multicarrier communication over underwater acoustic channels with nonuniform doppler shifts," *IEEE J. Ocean. Eng.*, vol. 33, no. 2, pp. 198–209, Apr. 2008.